UNIVERSITÀ DI PARMA
ARCHIVIO DELLA RICERCA

University of Parma Research Repository

On Performance Limits for Spectrally-Efficient Optical Transmission Techniques in Short-Haul Metro/Access Links",

note finali coverpage

(Article begins on next page)

02 February 2025

On Performance Limits for Spectrally-Efficient Optical Transmission Techniques in Short-Haul Metro/Access Links

Tommaso Foggi

Abstract—The demand for transmitting optical signals with high spectral efficiency (SE) by exploiting cost-effective systems and techniques is raising an increasing interest in the area of wide or metro area networks (WAN/MAN). Recently, many different solutions, e.g., amplitude modulation formats, direct-detection schemes, line coding, and simple signal processing techniques have been investigated for wavelength division multiplexing (WDM) short haul optical links, where coherent systems turn out to be economically unfavourable. In this paper the Time-Frequency Packing technique, already successfully proposed for long-haul coherent optical links, is extended to direct-detection systems, based on pulse amplitude modulation (PAM) and differential phase-shift keying (DPSK), with the purpose of trading between detection complexity and SE, and of providing performance limits for advanced digital signal processing (DSP) at the receive side.

Index Terms—Short-Haul,PON,Access,PAM4,DQPSK,LDPC,TFP

I. INTRODUCTION

THE recent growth of data traffic within the range of a few to tens of kilometers, i.e., inter/intra-datacenter interconnects and metro/access networks, has pushed the research towards optical systems that must be able to guarantee whether high spectral efficiency (SE), low latency, possibly low-complexity, and, consequently, cost-effectiveness. Hence, coherent optical systems, whose capacity has by now crossed the Terabit per second, by involving advanced transmission techniques and high-speed digital signal processing (DSP) in wavelength division multiplexing (WDM) solutions, are in this context replaced by simpler systems, basically exploiting intensity modulation direct detection (DD) or similar techniques. Nevertheless, one important aspect of future passive optical networks (PONs) is related to flexibility requirements; access networks based on PON architectures are intrinsically point-to-multipoint operating in limited power-budget scenarios, and, being typically based on time division multiplexing, the transmission is inherently in burst mode [1], [2]. Therefore, the need for more flexible solutions entail the employment of gradually more sophisticated DSP.

Many different approaches have been investigated in the latest years for short-haul passive PONs, all having in common simple detection schemes. Advanced modulation techniques were investigated, like high speed dual-polarization subcarrier modulation [3], [4], sideband modulation [5], high-order modulations with multi-tone transmission [6], or novel technologies [7]; alternatively, some processing was introduced at

transmit or receive side, like in the case of direct modulation, with or without electronic compensation [8]–[10], line coding [11] , Kramers-Kronig coherent detection [12], or even more sophisticated techniques based on machine learning [13]; eventually, combinations of these techniques were also proposed [14], [15], and many review papers have been published, where several of these candidate solutions were categorized and compared in terms of power efficiency and complexity [16]–[18].

In the light of increasing the SE and flexibility in short-haul links, the Time-Frequency Packing (TFP) technique [19], based on maximum a-posteriori probability (MAP) detection, is here proposed for DD coded, unamplified and uncompensated optical tranmission systems. TFP was initially introduced in optical communications for long-haul scenarios, since it can be fully exploited with coherent detection; yet, proper adaptations can make this technique suitable for DD schemes as well. Specifically, TFP is here tuned for both the simple and widespread on-off keying (OOK) modulation, and for quaternary pulse amplitude modulation (PAM), namely PAM4; then, it is also proposed for more sophisticated modulation formats, i.e., differential binary and quaternary phase-shift keying (DBPSK/DQPSK) with interferometric detection [20]. Binary and quaternary modulations are considered in this work, in order to simplify the technique presentation, but the same analysis and considerations also hold for higher-order modulations, e.g., multilevel PAM or differential multilevel PSK. The proposed DBPSK and DQPSK were proven to be extremely resilient to group velocity dispersion (GVD), as long as proper complexity of the MAP detector is taken into account, i.e., a sufficient number of trellis states [20]. Since TFP intrinsically exploits the MAP detection strategy, significant results can be intuitively achieved. Evidently, on the other hand a higher SE is provided at the price of a remarkable complexity increase at the receive side, if compared to standard DD. Although the presence of decoders can be considered common and unavoidable in current systems (please refer to [21] for insights on the complexity of the decoder), it must be considered that the complexity of the MAP detector scales exponentially with the number of interferers taken into account, but can be reduced by exploiting more sophisticated algorithms [22]. Moreover, iterative MAP detection entails latency issues that can be unacceptable in particular scenarios. However, the conventional trade-off between complexity and performance motivates the proposal of this powerful technique, that can eventually prove to be suitable for unforeseen appli-

cations, and, more practically, can provide useful benchmarks as concerns the performance limits of short-haul systems. In addition, TFP is intrinsically a flexible and burst-mode technique, that allows the adaptation of system parameters to fit the available resources, e.g., by adapting the code rate, transmit filter bandwidth and receiver complexity to the power budget at hand. Eventually, this technique was already successfully employed in experimental scenarios with OOK direct modulation [23], showing promising results.

II. SYSTEM MODEL AND CONSIDERED RECEIVERS

Fig. 1 shows the system model of the PAM system. Multiple streams of bits, properly encoded into low-density parity check (LDPC) codewords, possibly coming from different users, are mapped, through proper modulators, to ℓ streams of symbols $\mathbf{x}^{(\ell)} = (x_1^{(\ell)}, ..., x_{K-1}^{(\ell)})^T$ belonging to the PAM/DPSK constellations[1]; N_c carriers with frequency spacing equal to F are employed by parallel modulators to transmit the symbol streams on a single-mode fiber (SMF) link, then the signals are received by N_c independent detectors, upon optical filtering, whose purpose is to separate the channels. Optical amplification is not present, and only a single signal polarization is considered, given the short distance (as mentioned, a few tens of kilometers at most). Hence, the generic equivalent baseband signal at the corresponding receive side, before optical filtering and opto-electric conversion, reads

$$\sum_{k=0}^{K-1} x_k^{(\ell)} h(t - kT - \tau^\ell)e^{2\pi\ell(F+\Delta_\ell)t+\theta^\ell}, \quad (1)$$

where, T is the symbol time, $h(t)$ accounts for transmit filter $h_{TX}(t)$ and for the channel impulsive response $h_F(t)$, i.e., $h(t) = h_{TX}(t) * h_F(t)$,[2] τ^ℓ and θ^ℓ are the delay and initial phase of the ℓth carrier, and Δ_ℓ is the possible frequency offset. In the presented scenario, fiber propagation was only impaired by GVD, due to the short distances at hand. Therefore, being the system essentially linear, the amount of dispersion could be expressed as a function of symbol rate, namely

$$\gamma = 2\lambda_0 R D_r / \omega_0 \quad (2)$$

where ω_0 and λ_0 are the optical carrier frequency and wavelength, $R = 1/T$ is the symbol rate, and D_r is the residual fiber dispersion (in ps/nm). In the numerical results section, a reference symbol rate $R =$50 Gbaud was assumed, in order to provide results in a intuitive and immediate context. As a consequence, every other parameter value can be expressed as a function of this reference value. After propagation, the optical signal is converted to the electrical domain by an opto/electronic (O/E) front-end (different front-ends are used for DPSK systems, as shown in the following), sampled at symbol time, and, after frame synchronization, signal samples are processed by the MAP detector; finally, log-likelihood ratios (LLR) are iteratively exchanged between detector and decoder, in order to provide reliable decisions on the transmitted bits. In order to compute the trellis branch metrics during the detector iteration, a minimum mean square error (MMSE) algorithm is devised to provide accurate estimates of the intersymbol interference (ISI) coefficients, by exploiting known pilot symbols properly inserted at the beginning of each codeword. Following the TFP principle, the bandwidth of the transmit filter is chosen so as to intentionally introduce ISI in the system; in fact, the system optimization, i.e., filter bandwidths and frequency spacing, is performed by computing the information rate (IR), as will be explained in the next section.

Two main system families, within the framework of direct detection, are here analyzed. First, the popular PAM schemes, either binary (OOK), and quaternary (PAM4). In this case, as showed in Fig. 1, the opto-electric conversion is performed by a simple photodetector, therefore a square law trasformation affects the signal, and the phase information is lost. In the second case, DPSK modulation formats are considered, again either binary (DBPSK) and quaternary (DQPSK). Details on the relative detector will be given in following sections, but it is worth noting that these particular systems, besides being still based on direct detection, are able, if combined with proper detection algorithms, to exploit the phase information in order to completely, in theory, compensate for the GVD.

III. SPECTRAL EFFICIENCY ANALYSIS

The performance of the OOK/PAM4 systems can be usefully predicted by means of achievable lower bounds on the spectral efficiency[3]. An optical channel distorted by linear impairments is considered, and denoting by $\mathbf{y}$ a proper discrete-time sufficient statistic for the detection of information symbols $\mathbf{x} = \{x_k^{(\ell)}\}$, with size $N_c K$, the information rate, i.e., the average mutual information per symbol, can be defined as

$$\mathcal{I} = \lim_{K \to \infty} \frac{1}{2N_c K} E\left\{ \log_2 \frac{p(\mathbf{y}|\mathbf{x})}{\sum_{\mathbf{x}'} p(\mathbf{y}|\mathbf{x}')P(\mathbf{x}')} \right\} \left[\frac{\text{bit}}{\text{symbol}} \right] \quad (3)$$

where $E[\cdot]$ denotes expectation, $p(\cdot)$ a probability density function (PDF) and $P(\cdot)$ the probability mass function (PMF) of $\mathbf{x}$. Being the transmitted symbols independent and uniformly distributed from a given constellation, $P(\mathbf{x})$ is constant. Hence, the SE corresponds to the IR per unit bandwidth and time

$$\text{SE} = \frac{\mathcal{I}}{FT} \quad \text{[b/s/Hz]}$$

where FT represents the time-frequency slot occupied by the information symbol. Therefore, if F is decreased, I will be decreased as well due to interference, whereas the SE can possibly increase. By exploiting the auxiliary channel and mismatched detection principles, an achievable IR, and hence an achievable SE, symbolized as η, can be computed [19].[4] This technique, practically, consists in computing, by numerical methods, i.e. simulations, a different value for the

---

[1] In the following $(\cdot)^T$ denotes transpose and $(\cdot)^*$ complex conjugate.

[2] Notice that $h(t)$ could also account for any other filtering included in the transmitter, and $*$ denotes convolution.

[3] The DPSK systems, being nonlinear, as explained in the following, cannot be analyzed with this method.

[4] Achievable means that actually lower bounds on the true IR are computed, but these bounds are achievable by the employed detector, if proper coding is adopted or designed.
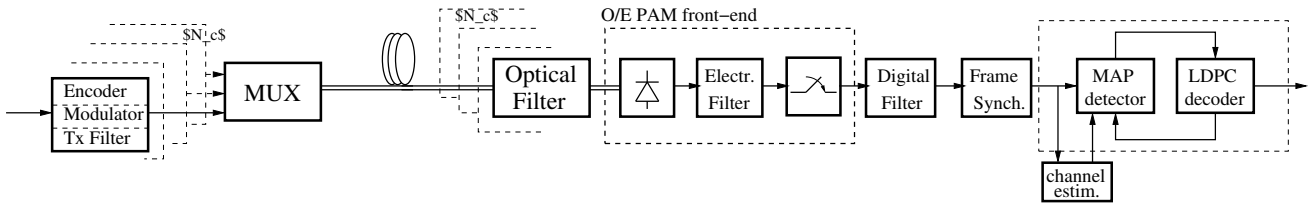
Figure 1: Schematic of the WDM PAM system.

information rate, that represents an achievable lower bound of the actual one,

$$\mathcal{I}_{LB} = \lim_{K \to \infty} \frac{1}{2N_c K} E \left\{ \log_2 \frac{q(\mathbf{y}|\mathbf{x})}{\sum_{\mathbf{x}'} q(\mathbf{y}|\mathbf{x}')P(\mathbf{x}')} \right\}, \quad (4)$$

where the PDFs $q(\mathbf{y}|\mathbf{x})$ and $q_p(\mathbf{y}) = \sum_{\mathbf{x}'} q(\mathbf{y}|\mathbf{x}')P(\mathbf{x}')$ are estimated by using the optimal MAP detector for the auxiliary channel law when it represents a finite-state channel, and replace the actual but unavailable[5] PDFs $p(\mathbf{y}|\mathbf{x})$ and $p(\mathbf{y}) = \sum_{\mathbf{x}'} p(\mathbf{y}|\mathbf{x}')P(\mathbf{x}')$ in (3). The optimal detector for the auxiliary channel, suboptimal for the true channel, will have the sequence $\mathbf{y}$ generated according to the actual channel model, as input, and the expectation in (4) is taken with respect to the input and output sequences generated accordingly [19]. Hence, the true statistics of the discrete-time received sequence are not required for the design of the adopted detector, which is designed for the auxiliary channel. If the auxiliary channel is changed, we obtain different lower bounds on the IR but, in any case, such bounds are achievable by those receivers. Each carrier is here detected by an independent receiver[6], which corresponds to the adoption of an auxiliary channel model that can be factorized into the product

$$q(\mathbf{y}|\mathbf{x}) = \prod_\ell q(\mathbf{y}^{(\ell)}|\mathbf{x}^{(\ell)})$$

where $\mathbf{y}^{(\ell)}$ is a proper discrete-time received sequence used for detection of symbols $\mathbf{x}^{(\ell)}$ transmitted over the ℓth carrier. Under this assumption, only one carrier, typically the central one which is the more affected by intercarrier interference (ICI), can be considered to provide results. The achievable lower bound on SE (achievable SE in the following), computed from the achievable IR with limited-complexity receivers, is thus

$$\eta_{\text{LB}} = \frac{1}{FT}\mathcal{I}_{\text{LB}} \quad [\text{b/s/Hz}]. \quad (5)$$

The auxiliary channel assumed for the MAP symbol detector design is based on the impulse response $h(t)$, i.e. it considers all channel effects, and the transmit and receive filters are optimized to obtain the best achievable SE, for each signal-to-noise ratio (SNR). A sufficient statistics $\mathbf{y}^{(\ell)}$ can be obtained by sampling the received pulse and it is possible to estimate the overall channel response (e.g., through a simple MMSE estimator) without any knowledge on the actual amount of

dispersion or filter bandwidths, which corresponds to the most practical way to design the MAP symbol detector. It is worth noting that this technique allows the computation of the achievable limit of the considered PAM receivers without taking into account specific coding schemes, being understood that, with a properly designed channel code, the information-theoretic performance can be closely approached. The performance of the DPSK, instead, cannot be predicted by exploiting the described method because the detectors are based on the per-survivor processing [24], which implies a feedback, therefore these receivers cannot be considered optimal neither for the auxiliary channel. As mentioned, the application of the TFP technique to direct-detection schemes, with respect to coherent ones, relies in the different signal model which deeply influences the design of the detector. In the following, the received signal model for both PAM and DPSK systems is given, showing the fundamental peculiarities of the proposed schemes, which entail different effects: the square-law detection in case of PAM, which leads to limited performances, and the interferometric differential detection of DPSK, which can be exploited to obtain remarkable results.

A. OOK/PAM4

The received signal in (1) after O/E conversion at the ℓth detector, i.e., square-law detection, reads

$$r(t) = |s(t)|^2 + w(t) = y^s(t) + w(t), \quad (6)$$

where $s(t) = \sum_{k=0}^{N-1} x_k^{(0)} h_r(t - kT - \tau^0)e^{\Delta_0 t + \theta^0}$, $h_r(t) = h(t) * h_{RX}(t)$ takes into account the presence of a receive side filter used to separate channels, so that only the central one is retained (so we have $\ell = 0$), and $w(t)$ represents the additive white Gaussian noise (AWGN) introduced by the electronic circuitry, with two-sided power spectral density equal to $N_0/2$. Then, by taking into account the filtering effect of the O/E front-end, $h_e(t)$, and sampling[7], the signal expression becomes

$$y_k = y_k^e + n_k = \sum_{m \leq j \leq L} x_m x_j f(m - k, j - k) + n_k, \quad (7)$$

with $n_k = w(t) * h_e(t)|_{t=kT}$, and $y_k^e = y^s(t) * h_e(t)|_{t=kT}$. Thus, the expression of the overall discrete-time system response can be modeled by a second-order Volterra kernel [25]

$$f(m, j) \doteq \int_{-\infty}^{+\infty} h_e(\tau) h_V(\tau + mT, \tau + jT)d\tau, \quad (8)$$

---

[5]Given the linear channel model here assumed, the actual PDFs could be available in some cases. However, in real systems, and even more so with TFP, not all the channel memory is usually taken into account at the receiver, therefore the IR of the true channel is often not available, since the optimal receiver is unknown or possibly of unmanageable complexity.

[6]Notice that intercarrier interference is not coped with.

[7]Please notice that further digital filtering after sampling, used for the optimization of FT, can be equivalently included in $h_e(t)$

where

$$h_V(t,s) \doteq \begin{cases} 2\Re[h_r(t)h_r^*(s)] & \text{for } t < s \\ |h_r(t)|^2 & \text{for } t = s \end{cases} \qquad (9)$$

where $\Re[\cdot]$ refers to the real component. Being L the true channel memory length, the $L_t = L(L+1)/2$ kernel coefficients can be effectively estimated by means of the MMSE algorithm. Clearly, a number of kernel coefficients smaller than L_t can be employed in the detector (so that $L_r < L$), in order to reduce its complexity, since the number of trellis states is equal to $S_r = M^{L_r}$ (with $M = 2, 4$), but at the expense of a worse performance. The branch metric for the MAP detector trellis computation is, in this case, the standard AWGN channel metric, but it can be simply modified to account for optical noise in amplified systems [26].

B. DUOBINARY

The quaternary duobinary system employed as a reference in the numerical results section is described in [11]. It is based on a in-phase/quadrature (IQ) modulator, so that the signal on each quadratures is modulated on three levels but with different gains. In this way a significant bandwidth saving can be obtained, and the direct detection of this signal still yields four levels, which can be discriminated by a simple threshold detector. This kind of line coding is part of the more general family of partial-response signalling [27], and it has been widely employed in both wireless and optical communications. In the presented results, a MAP detector with four states was employed to have a fair comparison with the proposed TFP solution.
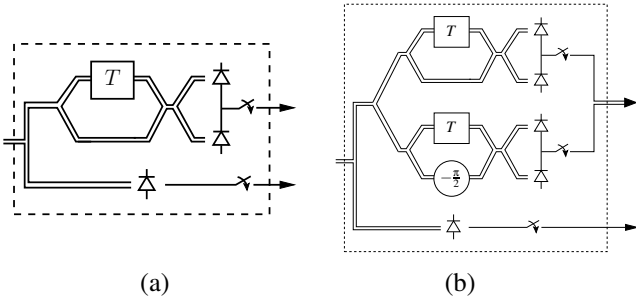
C. DBPSK/DQPSK

| (a) | (b) |

Figure 2: Schematics of the a) DBPSK and b) DQPSK O/E front-ends.

The second system family here proposed is based on an interferometric DD scheme; the symbol streams $\mathbf{x}^{(\ell)}$ are in this case also differentially encoded, and transmitted by a phase modulator, whereas the O/E front-end is now based on the interferometric principle, whose output expression, following a similar notation pattern as in (6)-(7), is

$$r(t) = s(t)s^*(t-T) + w(t) = z^s(t) + w(t), \qquad (10)$$

and, after sampling and by considering the front-end filtering

$$z_k = z_k^e + n_k. \qquad (11)$$

It is worth noting that the front-ends in Fig. 2 are specifically designed for the differential detection of a DBPSK and DQPSK respectively, therefore (10) is valid in both cases. As can be noticed, the DBPSK and DQPSK O/E front-ends also include an intensity photodetector, whose output is the same as in (7), that allows to employ an effective branch metric, as described in [20], that reads

$$\begin{aligned} \lambda_k(\mathbf{x}_{k-L_r}^k) &= \frac{1}{\sqrt{y_{k-1}}}[|z_k \hat{s}_k^*(\mathbf{x}_{k-L_r}^k) \\ &\quad + g_{k-1}| - |g_{k-1}|] - \frac{1}{2}|\hat{s}_k(\mathbf{x}_{k-L_r}^k)|^2, \end{aligned} \quad (12)$$

where

$$g_{k-1} = \alpha g_{k-2}z_{k-1}^*/y_{k-2} + y_{k-1}s_{k-1}^*(\mathbf{x}_{k-1-L_r}^{k-1}), \quad (13)$$

with α a proper step-size, and with $\hat{s}_k(\mathbf{x}_{k-L_r}^k)$ the sample estimates of the useful signal[8], $\hat{s}(t) = \sum_{k=0}^{N} x_k^{(0)} h_r(t - kT)$, depending on the previous L_r symbols, and y_k is the same as in (7). This branch metric, specifically conceived for phase noise compensation, was demonstrated to be particularly effective to cope with GVD, which indeed works as a phase distortion, and does not require a phase reference. In order to compute the recursive term g_{k-1} for each path in the trellis diagram, past signal samples are needed; hence, a per-survivor technique has been employed, as described in [24]. As opposite to the case of OOK/PAM4, the branch metric in (12) does not change if an optically amplified system is considered. In fact, in case of optically amplified links, the PAM signal model changes, as the channel cannot be considered AWGN anymore, and the branch metrics must be changed accordingly (see [26]), whereas in case of the proposed interferometric differential front-end, the noise statistics remain unchanged [20].

IV. NUMERICAL RESULTS

In order to measure the performance of the proposed receivers, 50 Gbaud transmission systems were simulated[9], and fiber propagation was considered for distances up to 50 km. In all simulations, only GVD was evaluated, with a dispersion parameter equal to 17 ps/nm/km, since for short-haul uncompensated links it entails the most detrimental channel impairment. Moreover, synchronization was assumed to be ideal. Non-return-to-zero (NRZ) pulses and ideal Mach-Zehnders (MZ) with infinite extinction ratio were assumed. At the transmit side, an electrical root-raised-cosine (RRC) filter with roll-off equal to 0.1 was assumed to drive the MZ and to shape the signal as to implement the TFP technique; only three independent channels were propagated ($N_c = 3$), since non-linear effects were neglected, and the achievable SE or bit-error rate (BER) were obtained from the central one.

[8]With the definition $\mathbf{x}_{k1}^{k2} \doteq (x_{k1}, x_{k1+1}, ..., x_{k2})^T$, given the integers $k2 > k1$.

[9]Please remember that all simulations were actually run by normalizing every physical parameter to the symbol time. The 50 Gbaud symbol rate was chosen in order to depict a popular scenario, as well as the chromatic dispersion typical of C-band transmissions. It bears repeating that other reference values can be chosen, thus obtaining, for instance, the lower chromatic dispersion of O-band, popular for short-reach links, and entailing different numerical results, but not different conclusions.

4

Distance	[km]	0	10	20
F	[GHz]	40	35	27.5
Tx LP RRC	[GHz]	22.5	21	20
Rx BP Gaussian	[GHz]	42.5	35	27.5
Rx LP RRC	[GHz]	22.5	21	20

Table I: PAM4 optimized frequency spacing F and filter 3-dB bandwidths, for achievable SE equal to 1: transmit (Tx) and receive (Rx) side low-pass (LP) and band-pass (BP) filters.

As mentioned, the frequency packing was tuned through the transmit electrical filter, whereas the bandwidth of a receive side 4th-order Gaussian optical filter was also optimized case by case, in order to cut side channels before photodetection, i.e., its bandwidth was set according to the frequency spacing. The same way an electrical 5th-order Bessel filter was used to model the transfer function of O/E front-end, with bandwidth equal to 35 GHz, and another RRC digital filter with roll-off equal to 0.1 was lastly designed to optimize the system performance. The optimization was thus performed by searching over a set of combined possible values of filter bandwidths and frequency spacings. An example of the optimized frequency spacing and bandwidths are given in Table I for PAM4, as a function of distance, and corresponding to an achievable SE equal to 1. It is worth specifying that, in this case, the optimized values are almost the same for both S_r equal to 4 and 16. Results are reported in terms of a proper SNR, so that a fair comparison can be outlined. The ratio between the signal and noise power (in the considered bandwidth), S/N, is taken as the SNR. It can be written as

$$S/N = \lim_{N_c \to \infty} \frac{N_c P_c}{B_0 2 N_0}, \quad (14)$$

where P_c is power for each carrier, B_0 the overall bandwidth. P_c is independent of the bandwidth B, and it is clearly $B_0 = (N_c-1)F+B$. In the limit of a large number of carriers (when border effects can be neglected or when B si comparable to F) the approximation $B_0 = N_c F$ holds and thus (see [19] for further details)

$$\frac{S}{N} = \frac{P_c}{2 N_0 F}. \quad (15)$$

All the following achievable SE and BER values were evaluated by simulating streams of 10^6 bits per channel, in order to obtain average values with a good confidence interval.

For the purpose of explaining the meaning and usefulness of achievable SE curves, Fig. 3 depicts the maximum achievable SE

$$\eta_M = \max_{F,B>0} \eta_{LB}(F, B) \quad (16)$$

computed in a OOK back-to-back configuration, i.e., without fiber propagation, and when the signal is propagated through 50 km of SMF, for different detector complexity, hence for increasing number of states S_r; it can be noticed that, in back-to-back, as soon as the detector complexity moves past the symbol-by-symbol configuration ($S_r = 1$), the performance increases remarkably, up to $\eta_M = 1.7$ for $S_r = 4 \div 8$. Then, results highlight the expected performance reduction when the fiber is present, although for $S_r = 8$ a maximum
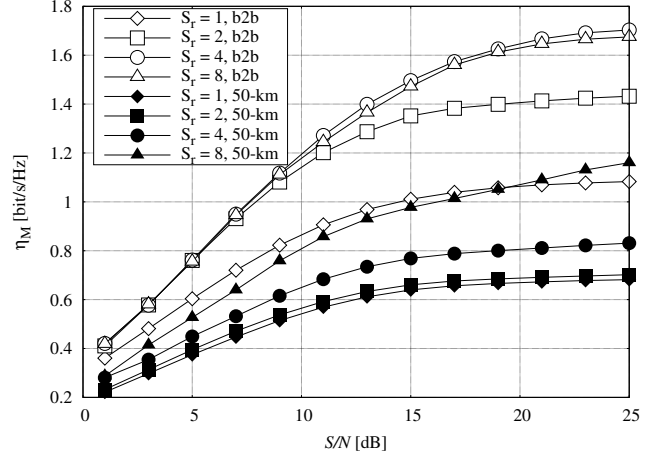

Figure 3: Maximum achievable spectral efficiency of the WDM OOK system in back-to-back (b2b) and after 50-km propagation, for increasing detector complexity.

achievable SE equal to 1.2 bit/s/Hz can still be reached. These predictions do not resort to any practical codes, therefore they are significantly faster than BER results to be obtained. It is worth noting that even if for each S/N step the optimization of filter bandwidths and channel frequency spacing F must be repeated, the optimal values are actually just slightly variable. Indeed, the optimization can be performed offline given a set of practical use cases, and the stored optimal values can be selected given the system at hand and the measured required parameters, e.g, the SNR.

By extending the previous analysis to intermediate distances, more exhaustive results can be provided. The performance of the receivers are also evaluated through BER simulations, by employing LDPC codes tailored to the specific scenario[10], with code length equal to 64800 bits and code rates appropriately chosen according to the computed achievable IR. Basically, the achievable IR values represent the ideal rate of the code to be employed to reach the bound, that is, obtaining an error-free transmission for the specified SNR, however, considered the non-ideality of practical codes, usually lower code rates and higher SNRs must be used to approach the expected performance. The simulation results shown in the following figures refer to the SNR corresponding to a BER value equal to 10^{-4}, that represents a proper simulation threshold, since these codes have a steep waterfall, so that lower BERs, down to $10^{-7} \div 10^{-8}$, can be reached with a SNR value of just a fraction of dB higher.[11] In the following figures each point represent the performance obtained with the labeled combination of code rate and number of trellis states, considering a maximum number of iterations equal to 20 with detection and decoder updates performed at every iteration. As previously mentioned, the achievable IR for DPSK formats cannot be computed, therefore the SE optimization was attained by

---

[10]The progressive-edge-growth (PEG) algorithm was used to design the codes [28].

[11]LDPC codes are known to often show BER floors that can hardly be simulated, being usually below 10^{-6}. These performance limits can be bypassed by adding and external code, for instance a BCH code, which allow the reduction of the BER below 10^{-12}, see [29] for details.
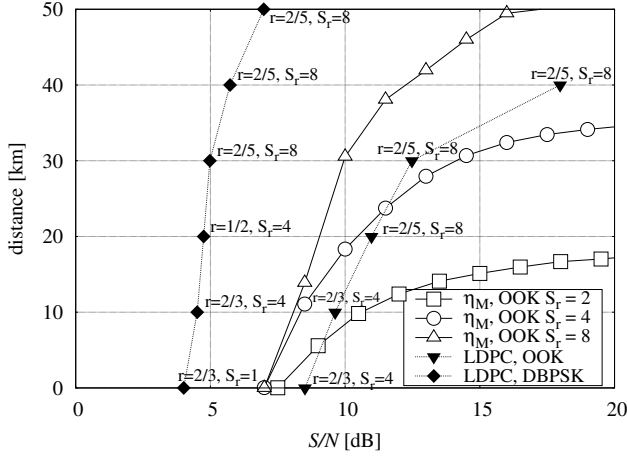
Figure 4: Contour plots of binary modulations for η_M equal to 1 bit/s/Hz, as a function of S/N and distance, and BER results of LDPC coded simulations with variable code rates and detector complexities.

Figure 5: Contour plots of binary modulations for η_M equal to 1.5 bit/s/Hz, as a function of S/N and distance, and BER results of LDPC coded simulations with variable code rates and detector complexities.

Figure 6: Contour plots of quaternary modulations for η_M equal to 1 bit/s/Hz, as a function of S/N and distance, and BER results of LDPC coded simulations with variable code rates and detector complexities. The performance of IQ-duobinary is also included.

means of the BER performance. Fig. 4 shows the contour plots for $\eta_M = 1$ bit/s/Hz, as a function of SNR and distance for binary modulations. The expected performance, as stated by the achievable SE curves, can be approached with good accuracy by proper combination of code rates and detector complexity, following the receiver parameter configuration suggested by the achievable SE curves themselves. Fig. 5 presents the contour plots for $\eta_M = 1.5$ bit/s/Hz; in this case, the OOK receiver maximum reach stops at about 20 km for 22.5 dB, as predicted by the flat achievable SE curve, whereas the DBPSK receiver more than double this distance at lower SNR, by reaching a distance of 50 km for 21 dB. It must be noticed that for short distances, the OOK detector performs better for $S_r = 4$ than for $S_r = 8$; this behaviour can be explained by the particular ISI configuration, because a non minimum-phase ISI channel, which imply that the energy is not concentrated in the first coefficients, can cause this kind of results when not all the channel memory is taken into account at the receiver, as explained in [24]. Clearly, intermediate results for $1 \leq \eta_M \leq 1.5$ can be easily envisaged. Then, Figs. 6-7 show results on the quaternary modulation formats. The performance of IQ-duobinary was also included to highlight the gap with respect to optimized TFP. These curves still refer to $\eta_M = 1.$ and $\eta_M = 1.5$ bit/s/Hz, respectively, but only for PAM4 and IQ-duobinary, whereas the DQPSK results refers to a doubled spectral efficiency (SEx2), therefore stressing a remarkable performance increase. It is also worth stressing the gap between the nominal SE of these quaternary modulation formats, i.e. 2 b/s/Hz, and the actual one, computed by taking into account all significant parameters. The achievable SE is again followed quite accurately by BER results for PAM4, and a significant improvement can be noticed with respect to IQ-duobinary in both figures. The DQPSK results, only expressed in terms of LDPC performance, since, as previously mentioned, it is not possible to compute achievable lower bound for these suboptimal detectors, were obtained by optimizing the spacings and bandwidths through BER evaluation, and suggest
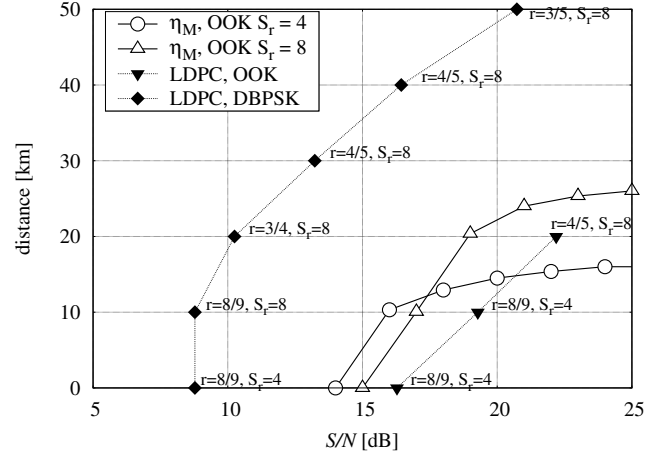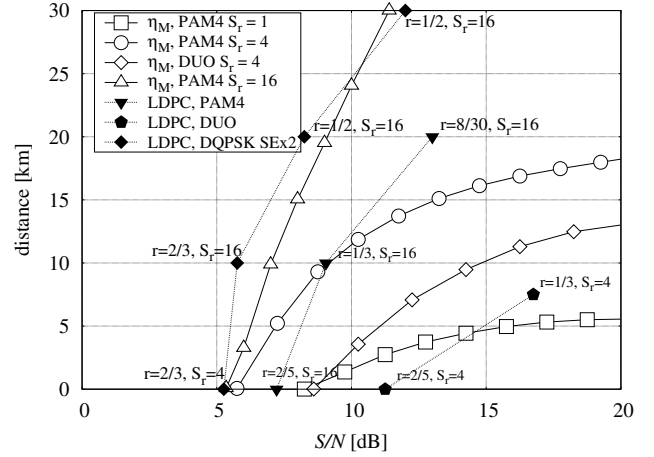
a wide margin to trade between the two metrics represented by performance and complexity.

V. CONCLUSION

TFP was proposed with two binary and two quaternary direct detection systems, namely OOK and DBPSK, PAM4 and DQPSK, and its performance evaluated for short-haul uncompensated and unamplified optical links. Results demonstrate that the system SE, or conversely the propagation distance, can be considerably improved through TFP, despite it clearly entails a significant receiver complexity increase. In particular, the performance gap between PAM4 and DQPSK is remarkable, even if at the cost of a significant complexity increase. In this light, a convenient trade-off between performance and complexity could be enabled by specific unforeseen use cases, although the low-latency and cost-effectiveness constraints on

Figure 7: Contour plots of quaternary modulations for η_M equal to 1.5 bit/s/Hz, as a function of S/N and distance, and BER results of LDPC coded simulations with variable code rates and detector complexities. The performance of IQ-duobinary is also included.
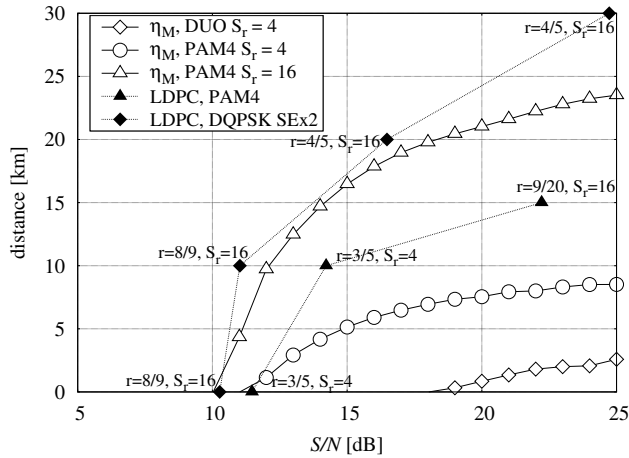
short-haul systems, at the present time, seem to prevent the employment of such technique in most cases. In any case, the DPSK schemes represent a benchmark for direct detection systems, showing that better performance can be obtained if more advanced DSP techniques are employed. Eventually, the presented results, obtained for unamplified links, can be easily extended to amplified systems (the DPSK detectors and DSP do not even need any modifications).

References

[1] X. Liu and F. Effenberger, "Emerging optical access network technologies for 5G wireless [invited]," *IEEE/OSA Journal of Optical Communications and Networking*, vol. 8, pp. B70–B79, December 2016.

[2] D. van Veen and V. Houtsma, "Digital signal processing in optical access systems," in *OSA Advanced Photonics Congress (AP) 2019 (IPR, Networks, NOMA, SPPCom, PVLED)*, p. SpT1E.1, Optical Society of America, 2019.

[3] J. C. Cartledge and A. S. Karar, "100 Gb/s intensity modulation and direct detection," *J. Lightwave Technol.*, vol. 32, pp. 2809–2814, Aug. 2014.

[4] M. S. Erkılınç, Z. Li, S. Pachnicke, H. Griesser, B. C. Thomsen, P. Bayvel, and R. I. Killey, "Spectrally efficient WDM nyquist pulse-shaped 16-QAM subcarrier modulation transmission with direct detection," *J. Lightwave Technol.*, vol. 33, pp. 3147–3155, Aug. 2015.

[5] H.-C. Chien, J. Zia, J. Zhang, Z. Dong, and J. Yu, "Optical independent-sideband modulation for bandwidth-economic coherent transmission," *Opt. Express*, vol. 22, pp. 9465–9470, Apr. 2014.

[6] A. Dochhan, H. Griesser, N. Eiselt, M. H. Eiselt, and J.-P. Elbers, "Solutions for 80 km DWDM systems," *J. Lightwave Technol.*, vol. 34, pp. 491–499, Jan. 2016.

[7] H. Mardoyan, F. Jorge, O. Ozolins, J. M. Estaran, A. Udalcovs, A. Konczykowska, M. Riet, B. Duval, V. Nodjiadjim, J. Dupuy, X. Pang, U. Westergren, J. Chen, S. Popov, and S. Bigo, "204-Gbaud on-off keying transmitter for inter-data center communications," in *2018 Optical Fiber Communications Conference and Exposition (OFC)*, pp. 1–3, Mar. 2018.

[8] D. Che, A. Li, X. Chen, Q. Hu, and W. Shieh, "Rejuvenating direct modulation and direct detection for modern optical communications," *Optics Communications*, vol. 409, pp. 86 – 93, 2018.

[9] S. Ohlendorf, R. Joy, S. Pachnicke, and W. Rosenkranz, "Optimizing reach and capacity of IM/DD systems by using multidimensional PAM and DSP," in *Advanced Photonics 2018 (BGPP, IPR, NP, NOMA, Sensors, Networks, SPPCom, SOF)*, p. SpTh2G.2, Optical Society of America, 2018.

[10] H. Y. Rha, S. Moon, H. Kang, S. Lee, I. Hwang, and J. K. Lee, "Low-complexity soft-decision viterbi algorithm for IM/DD 56-Gb/s PAM-4 system," *IEEE Photonics Technology Letters*, vol. 31, pp. 361–364, Mar. 2019.

[11] M. Chagnon, T. A. Eriksson, R. Dischler, F. Buchali, H. Bülow, and S. ten Brink, "Duobinary IQ modulation schemes for C- and O-band PAM4 direct detect systems," in *2017 European Conference on Optical Communication (ECOC)*, pp. 1–3, Sep. 2017.

[12] A. Mecozzi, C. Antonelli, and M. Shtaif, "Kramers–kronig coherent receiver," *Optica*, vol. 3, pp. 1220–1227, Nov. 2016.

[13] A. Argyris, J. Bueno, and I. Fischer, "Photonic machine learning implementation for signal recovery in optical communications," *Scientific reports*, vol. 8, p. 8487, May 2018.

[14] Z. Liu, B. Kelly, J. O'Carroll, R. Phelan, D. J. Richardson, and R. Slavík, "Discrete multitone format for repeater-less direct-modulation direct-detection over 150 km," *J. Lightwave Technol.*, vol. 34, pp. 3223–3229, Jul. 2016.

[15] D. Sadot, G. Dorman, A. Gorshtein, E. Sonkin, and O. Vidal, "Single channel 112 Gbit/sec PAM4 at 56Gbaud with digital signal processing for data centers applications," *Opt. Express*, vol. 23, pp. 991–997, Jan. 2015.

[16] M. Sharif, J. K. Perin, and J. M. Kahn, "Modulation schemes for single-laser 100 Gb/s links: Single-carrier," *J. Lightwave Technol.*, vol. 33, pp. 4268–4277, Oct. 2015.

[17] J. K. Perin, A. Shastri, and J. M. Kahn, "Data center links beyond 100 Gbit/s per wavelength," *Optical Fiber Technology*, vol. 44, pp. 69 – 85, 2018. Special Issue on Data Center Communications.

[18] K. Zhong, X. Zhou, J. Huo, C. Yu, C. Lu, and A. P. T. Lau, "Digital signal processing for short-reach optical communications: A review of current technologies and future trends," *Journal of Lightwave Technology*, vol. 36, pp. 377–400, Jan. 2018.

[19] G. Colavolpe and T. Foggi, "Time-frequency packing for high capacity coherent optical links," *IEEE Trans. Commun.*, vol. 62, pp. 2986–2995, Aug. 2014.

[20] G. Colavolpe, T. Foggi, E. Forestieri, and G. Prati, "Multilevel optical systems with MLSD receivers insensitive to GVD and PMD," *J. Lightwave Tech.*, vol. 26, pp. 1263–1273, May 15 2008.

[21] H. Wymeersch, H. Steendam, and M. Moeneclaey, "Log-domain decoding of LDPC codes over GF(q)," in *2004 IEEE International Conference on Communications (IEEE Cat. No.04CH37577)*, vol. 2, pp. 772–776 Vol.2, June 2004.

[22] G. Colavolpe, D. Fertonani, and A. Piemontese, "SISO detection over linear channels with linear complexity in the number of interferers," *IEEE J. Sel. Topics in Signal Proc.*, vol. 5, pp. 1475–1485, Dec. 2011.

[23] A. Malacarne, F. Fresi, G. Meloni, T. Foggi, and L. Potì, "Time-frequency packed VCSEL-based IM/DD transmission for WDM access networks," in *2016 21st OptoElectronics and Communications Conference (OECC) held jointly with 2016 International Conference on Photonics in Switching (PS)*, pp. 1–3, Jul. 2016.

[24] D. Fertonani, A. Barbieri, and G. Colavolpe, "Reduced-complexity BCJR algorithm for turbo equalization," *IEEE Trans. Commun.*, vol. 55, pp. 2279–2287, Dec. 2007.

[25] W. Chung, "Channel estimation methods based on Volterra Kernels for MLSD in optical communication systems," *IEEE Photonics Technology Letters*, vol. 22, pp. 224–226, Feb. 2010.

[26] T. Foggi, E. Forestieri, G. Colavolpe, and G. Prati, "Maximum likelihood sequence detection with closed-form metrics in OOK optical systems impaired by GVD e PMD," *J. Lightwave Tech.*, vol. 24, pp. 3073–3087, Aug. 2006.

[27] P. Kabal and S. Pasupathy, "Partial-response signaling," *IEEE Transactions on Communications*, vol. 23, pp. 921–934, Sep. 1975.

[28] H. Xiao and A. H. Banihashemi, "Improved progressive-edge-growth (PEG) construction of irregular LDPC codes," *IEEE Commun. Letters*, vol. 8, pp. 715–717, Dec. 2004.

[29] M. Secondini, T. Foggi, F. Fresi, G. Meloni, F. Cavaliere, G. Colavolpe, E. Forestieri, L. Potì R. Sabella, and G. Prati, "Optical time-frequency packing: Principles, design, implementation, and experimental demonstration," *Journal of Lightwave Technology*, vol. 33, pp. 3558–3570, Sep. 2015.